Measurement of the Fine Structure Separation $3\,^3P_1-3\,^3P_2$ for the Helium Atom*

W. E. LAMB, JR.,† AND T. H. MAIMAN‡
Stanford University, Stanford, California
(Received August 1, 1956)

The fine structure of helium levels $(1s3p)\,^3P_J$, $J=1$, 2 is determined by the microwave-optical method outlined in the preceding paper. Helium atoms are excited to $3\,^3P_J$ by electron bombardment and the optical radiation $3\,^3P_J\rightarrow 2\,^3S_1$(3889 A) is observed with a photomultiplier tube. The intensity of this radiation changes when radio waves induce transitions between the fine structure sublevels. The separation $3\,^3P_1-3\,^3P_2$ is found to be 658.0±1.0 Mc/sec, which is to be compared to the most recent optical estimates of 750±300 Mc/sec.

I. INTRODUCTION

IN the preceding article,[1] a method was proposed for making microwave measurements of the fine structure of excited atoms. This paper describes the first experimental realization of the method, and gives some early results of measurement on the fine-structure separation $3\,^3P_1-3\,^3P_2$ of helium. Work dealing with other and more accurate measurements will be published later.

In principle, the proposed scheme, as indicated in Fig. 1, is very simple. The atomic states to be studied are excited by electron bombardment of the gas, and the intensity of light emitted in their decay is measured. An electromagnetic field applied to the excited atoms causes a change in intensity and polarization of the light when the radio-frequency corresponds to the energy separation of two fine-structure states.

II. EXPERIMENTAL CONSIDERATIONS

1. Choice of Transitions

In Sec. XIII of the preceding paper,[1] it was estimated that one might expect 10^{-9} w of optical radiation $2\,^3P\rightarrow 2\,^3S$(10 830 A) or $3\,^3P\rightarrow 2\,^3S$(3889 A) into a detector. Since photomultipliers are far more sensitive for 3889 A than for 10 830 A, the first resonances were obtained for the $3\,^3P$ states. Earlier efforts to work with the $2\,^3P$ states were frustrated by the low sensitivity, high dark current, and instability of available infrared sensitive photomultipliers, as well as by the presence of a large amount of infrared background light from the filament of the electron gun. It is hoped that these obstacles can be overcome now that the apparatus is working properly for the $3\,^3P$ resonances.

It was shown in the preceding paper[1] that there were some 20 possible transitions between the fine-structure sublevels of $3\,^3P$. Since the first goal was measurement of the separation $\Delta E=E_1-E_2$, transitions like those numbered "1" through "8" in Table III of reference 1, whose frequencies are most dependent on ΔE, are to be preferred to the other transitions. At a magnetic field parameter $x=1$ ($H\sim 470$ gauss), the transitions in order of decreasing rf matrix element V [reference 1, Eq. (29)] are "3", "2", "1", "4", "5" with "6", "7", and "8" too weak to be considered. The intensity factors $\Delta|\mathfrak{d}|^2\Delta\sigma$ [reference 1, Eq. (34)] favor transitions in the order "5", "6", "2", "8", "4", "1" with "3" and "7" very weak. On the basis of these calculations, the choice of the most suitable resonance for study would seem to lie between transitions "2" and "5." For 50% saturation, "5" would be two times as intense as "2", but would require twice as much rf magnetic-field amplitude. Various requirements of rf and optical design tended to favor the choice of transition "5" for the first attempts. The dependence of its frequency on magnetic field is shown in Fig. 2, or in the more complete Fig. 11 of reference 1.

2. Background Current and Signal-to-Noise Ratio

The photocell current arises not only from the radiation $3\,^3P\rightarrow 2\,^3S$, but also from thermionic emission, helium radiation other than 3889 A, and stray filament light. The last two could be greatly reduced by an optical filter. The dark current of the photomultiplier (RCA 6199), even without cooling, was small compared to the current due to 3889 A radiation. The largest contribution to background light arises from that part (90% according to Sec. X of reference 1, and in practice, more) of the 3889 A radiation which cannot be affected by rf transitions.

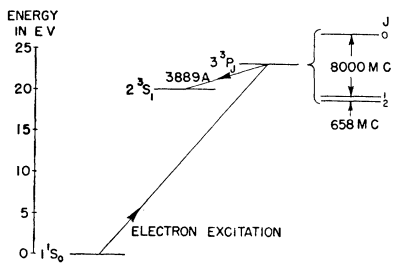

FIG. 1. Microwave optical method applied to the triplet fine structure of helium. Electron bombardment excites the sublevels unequally. The intensity of 3889A radiation emitted in decay to $2\,^3S_1$ can be changed by rf-induced redistribution among the sublevels.

* This work was supported in part by the joint program of the Office of Naval Research and the U. S. Atomic Energy Commission. The paper is based on a thesis submitted by T. H. Maiman in partial fulfillment of the requirements for the degree of Doctor of Philosophy in Physics at Stanford University.

† Present address: Clarendon Laboratory, University of Oxford, Oxford, England.

‡ Present address: Hughes Research and Development Laboratories, Culver City, California.

[1] W. E. Lamb, Jr., Phys. Rev. **105**, 559 (1957), preceding paper. A brief account of this work was reported in Phys. Rev. **98**, 1194(A) (1955).

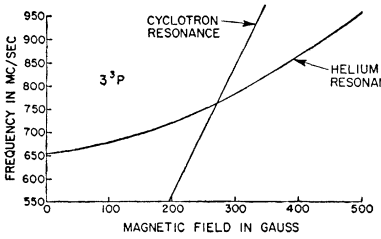

FIG. 2. Frequencies of transition "5" and electron cyclotron resonance as functions of magnetic field.

With power of 10^{-9} w, the number of 3889 A photons per second reaching the photocathode is 2×10^9. For a quantum efficiency of 10% (S-4 photosurface), the primary photocurrent is 2×10^8 electrons per second.

Any fluctuations in photomultiplier current constitute a source of noise. The largest contribution to this noise is simply shot noise at the photocathode. For a large number n of electrons emitted independently, the rms fluctuation is $n^{\frac{1}{2}}$. The rms noise current, averaged for a time τ, is then

$$i=\sqrt{n}\,e/\tau=(Ie/\tau)^{\frac{1}{2}}, \tag{1}$$

where

$$I=ne/\tau \tag{2}$$

is the average photocathode current. The (useful) signal is

$$S=\alpha GI, \tag{3}$$

where G is the photomultiplier gain and α is the fractional change in photocurrent at the peak of an rf resonance. The signal-to-noise ratio is

$$S/N=\alpha(\tau I/e)^{\frac{1}{2}}. \tag{4}$$

In practice, α was found to be of the order 0.3% (compared to 10% "expected"). Taking $I/e=2\times10^8$ electrons per second, and time constant[2] $\tau=3$ sec, one finds $S/N=73$. Allowing an increase[3] in N by 25% for fluctuations in the number of incident photons and for noise associated with secondary multiplication, the expected signal-to-noise ratio becomes $S/N=59$, as compared to an observed value of about 50.

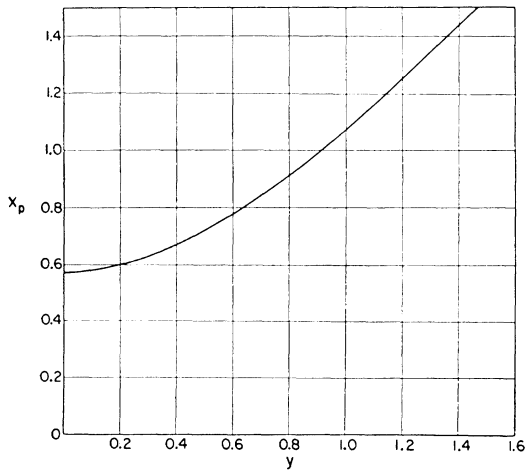

FIG. 3. Plot of x_p against y shows how abscissa of resonance peak varies with modulation amplitude.

[2] For an RL circuit shunted by a capacitance C, the effective time constant is $\tau=\frac{1}{2}RC$. For example, R. Becker, *Theorie der Elektrizität* (B. G. Teuber, Berlin, 1933), Vol. 2, pp. 6–13.

3. Detection of Resonance

The most obvious method for detection of resonances is to measure the change of photomultiplier current produced by rf fields for various frequencies. The expected resonances have a width[4] at half-height of about 4 Mc/sec, and one could vary frequency through a band of that width centered at 658 Mc/sec while keeping the amplitude of rf magnetic field fairly constant. For reasons that have become familiar, it was more convenient to keep the frequency constant and to vary the Zeeman splitting of the levels in an applied magnetic field. Difficulties with this direct current method would, however, arise from drifts and instabilities. In order to realize the signal-to-noise ratio quoted above, it would be necessary to reduce the magnitude of these effects to a value lower than noise level, which in operation was about 0.01% of the total background. Hence bombarding current, intensity of collision light, and photomultiplier gain must be stable to one part in 10^4. Even if these severe requirements were met, operation would be very inconvenient. Any changes in settings of bombardment voltage or current, photomultiplier gain, etc., would drive the indicating meter far off scale.

4. Modulation Methods

In view of these detection difficulties, a method involving modulation has great advantages. One of the resonance parameters is subjected to a small periodic variation which causes the photomultiplier output to have a time-varying component of current. An amplifier responsive only to a narrow band of frequencies centered at the fundamental frequency of modulation can then be used to detect the resonance as the applied magnetic field is slowly swept.

Resonance parameters available for modulation include (1) amplitude of rf, (2) oscillator frequency, and (3) magnetic field strength. Any one of these methods can give a spurious signal due to disturbance of the electron beam which produces the collision light.

It was estimated in Sec. X of reference 1 that an rf magnetic field of 5.6 gauss is required for 50% saturation of resonance "5." Even though such an rf magnetic field would, in itself, have little effect on the electron beam, it is impossible to avoid the presence of a superimposed rf electric field if the electron beam has a finite cross-sectional area. In the apparatus described below, this rf electric field effect was at least ten times

[3] G. A. Morton, RCA Rev. **10**, 525 (1949).

[4] Reference 1, Sec. X.

larger than the strongest triplet helium resonance. This tended to rule out the method of rf amplitude modulation.

Frequency modulation was not easily practicable here. In order to obtain a sufficiently large rf magnetic field from available oscillators it was necessary to place the gas sample in a resonant cavity whose Q was several times larger than that of the helium resonance. Frequency modulation of the oscillator would then lead to amplitude modulation of the applied rf fields and the difficulties of the previous method.

Magnetic field modulation tends to give some anomalous photomultiplier output due to disturbance of the electron beam. Fortunately this effect can be greatly reduced by a feedback beam-current regulator described below.

5. Analysis of Magnetic Field Modulation Method

In order to facilitate detection of resonances, the magnetic field was swept through a few gauss at a frequency of $1000/7\sim143$ cps. Of the various types of modulation wave form which can be used, a square wave gives the highest signal-to-noise ratio, and makes analysis of resonance shape simple.

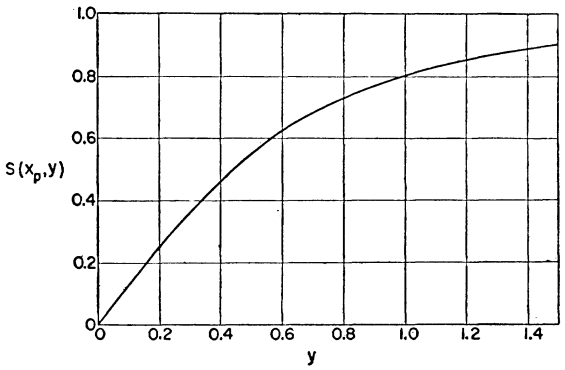

FIG. 4. Plot of resonance height $S_{\max}(y)$ against modulation-amplitude parameter y.

For a Lorentzian resonance curve

$$F(x)=1/(1+x^2), \tag{5}$$

where

$$x=(H-H_R)/\Delta H \tag{6}$$

measures the departure from resonance field H_R in units of the half-width at half-height ΔH, with square-wave modulation of amplitude $y\Delta H$, the chart response is proportional to

$$S(x,y)=F(x-y)-F(x+y), \tag{7}$$

which has the appearance of a dispersion curve. The peaks of $S(x,y)$ occur where $\partial S/\partial x=0$, or for $x=x_p$ given by

$$x_p^2=-\tfrac{1}{3}(1-y^2)+\tfrac{2}{3}(1+y^2+y^4)^{\frac{1}{2}} \tag{8}$$

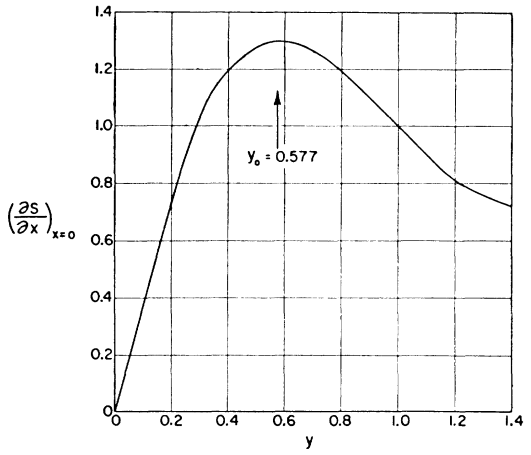

FIG. 5. Plot of slope of resonance curve at center as a function of modulation-amplitude parameter y.

and plotted in Fig. 3. The peak height $S(x_p,y)$ is plotted as a function of y in Fig. 4.

The resonance occurs when the curve $S(x,y)$ crosses the base line, i.e., at $x=0$ for any modulation amplitude parameter y. The sensitivity of such a determination is proportional to the value of $(\partial S/\partial x)_{x=0}$ which is plotted in Fig. 5. The optimum sensitivity at resonance occurs for

$$\frac{\partial}{\partial y}\left(\frac{\partial S}{\partial x}\right)_{x=0}=0, \tag{9}$$

or for $y=y_0=(1/3)^{\frac{1}{2}}$. Under these conditions, the peak-to-peak separation in x has increased by 31.8% over its small modulation value.

III. APPARATUS

A block diagram of the apparatus is shown in Fig. 6, and the separate components are described below.

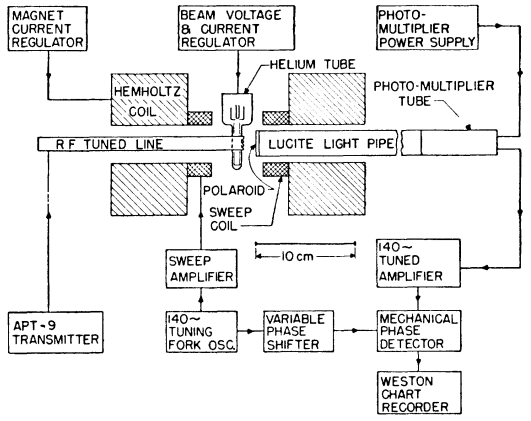

FIG. 6. Block diagram of apparatus used for microwave-optical study of excited atoms.

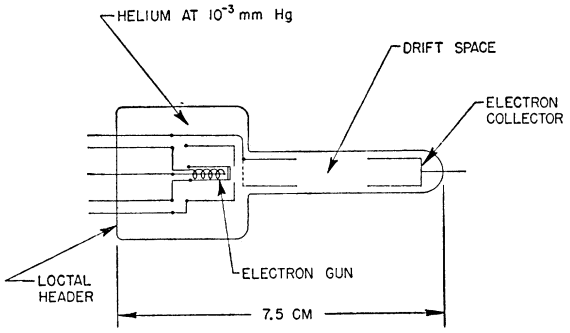

FIG. 7. Helium excitation tube.

1. Excitation Tube

After much preliminary work with a continuously pumped system,[5] a sealed-off excitation tube was used, as shown in Fig. 7. This has an oxide-coated "L" cathode, a control electrode for beam current variation, an accelerating electrode for establishing the beam energy, a drift region "free" of electric fields, and an electron collector. Helium pressure in the tube was about 3×10^{-3} mm. "Clean-up" did not occur because the tube was operated at this pressure on a pumping station before seal-off. Because of space charge effects, the tube required an axial magnetic field to confine the electron beam.

2. Tube Power Supply

As noted previously, magnetic field modulation tends to modulate the electron beam in the excitation tube.

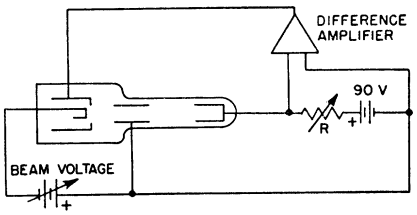

FIG. 8. Beam-current regulator. In an equilibrium condition, the input to the difference amplifier is very small (ideally zero), and hence the voltage drop across R is $E=90$ v. If a disturbance occurs (such as a change in magnetic field), the beam current might increase and cause an increase in the potential across R. The amplifier output polarity is such that an increase in beam current would make the control electrode go more negative and the beam current is reduced towards its equilibrium value. The gain of the amplifier is high (about 10^4) so that the amplifier input is always small. The voltage drop across R and hence the beam voltage remains approximately constant. If, for instance, the change in magnetic field required a change in the control electrode potential by 10 v to keep the beam current constant, the potential across R would change by only $10/10^4$ v or by 0.001%.

[5] In some of this work, the rf leads were brought into the vacuum envelope. Serious trouble was then experienced with an rf breakdown designated as "multipactor" effect in the klystron work. See W. G. Abraham "Interactions of electrons and fields in cavity resonators," Ph.D. thesis, Stanford University, June, 1950 (unpublished). Also, E. W. B. Gill and A. von Engel, Proc. Roy. Soc. (London) **192**, 446 (1947).

In order to counteract this effect, a beam-current regulator was incorporated in the tube power supply. Its operation can be understood by reference to Fig. 8. The current regulator is effective also against other disturbances such as variations of cathode emission and beam voltage. The latter property is useful when taking excitation curves.

3. Magnet and Supply

The magnetic field for the helium tube was supplied by a pair of Helmholtz coils capable of providing fields up to 600 gauss. At maximum field, the current required was 1.25 amp. In normal operation the field ranged from 350 to 600 gauss. The magnet current was stabilized to a few parts in 10^5 by use of a circuit (shown in Fig. 9) which is based on that of a conventional feedback regulator.

The modulation magnetic field was produced by separate Helmholtz coils driven by a square-wave generator. It was shown by observing the modulated magnetic field with a loop probe and oscilloscope that the wave form of the field was closely square wave.

4. Photomultiplier and Optical System

The 3889 A radiation was detected by an RCA 6199 photomultiplier tube. In order to realize the full sensitivity of the photosurface, it was necessary to reduce stray magnetic fields to about 0.1 gauss. This was accomplished by placing the photomultiplier tube out of the main field and using a Lucite light pipe for optical coupling. In addition, the photomultiplier was encased in a μ-metal shield.

In order to reduce light from the filament, and from spectral lines of helium other than 3889 A, it was planned to use a narrow-band interference filter centered at 3889 A. It turned out that a piece of blue glass which

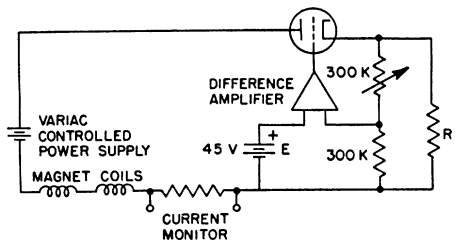

FIG. 9. Magnet current regulator. The voltage drop across the reference resistor R is maintained constant, and apart from the voltage-divider ratio, equal to the reference battery potential E. Except for the small voltage-divider current, the magnet current and reference resistor current are equal. The temperature coefficient of the reference battery and reference resistor were both positive and of the same order of magnitude (30 ppm/deg C). Since the magnet current is proportional to E/R, variation in current with ambient temperature was small. The measured value was about 5 ppm/deg C. The difference amplifier had a short time ($\sim$10 min) stability of about 10^{-3} volt, and hence the fractional instability in current due to this cause was $10^{-3}/45$ or about 20 ppm. The short-time stability measured with a potentiometer was of this order of magnitude.

cut off wavelengths longer than about 4000 A was sufficient. The nearby helium line 3965 A was not strongly excited[6] below 40-ev bombardment energy. A polaroid sheet (without ultraviolet absorber) was placed in the optical system, and could be rotated to determine the degree of polarization of the helium light.

5. Amplifier and Phase Detector

The narrow band width needed to attain the signal-to-noise ratio given in Sec. II2 was achieved with a tuned amplifier-phase detector combination. The amplifier was tuned to the modulated frequency 1000/7 cps with a toroidal choke in a Q-multiplier circuit[7] giving a band width of about 0.7 cps. A mechanical chopper was employed as a phase detector in a full-wave synchronous rectifier circuit. A mechanical detector was selected to avoid balancing controls and higher-order interaction responses associated with most vacuum-tube phase detector circuits. The band width was limited by a three-second RC time constant in the output of the phase detector, giving an over-all noise band width of about 0.16 cps. The resonances were displayed on a Weston chart recorder connected to the output of the phase detector.

6. Radio-Frequency System

In order to be able to apply sufficient rf magnetic field to the helium with a reasonable power output from the jammer transmitter, the excitation tube was placed inside a resonant cavity shown in Fig. 10, which consisted of a tuned parallel-strip transmission line operating in its half-wavelength mode. This tuned line was placed inside a section of S-band wave guide which merely served as a radiation shield. The end of the transmission line was shorted so that the helium would be acted on primarily by an rf magnetic field, and was slotted in order to allow the helium light to escape in a direction at right angles to the direction of electron bombardment. This rf field configuration favored π transitions, but there were sufficient amounts of perpendicular components of field to induce some of the stronger σ transitions.

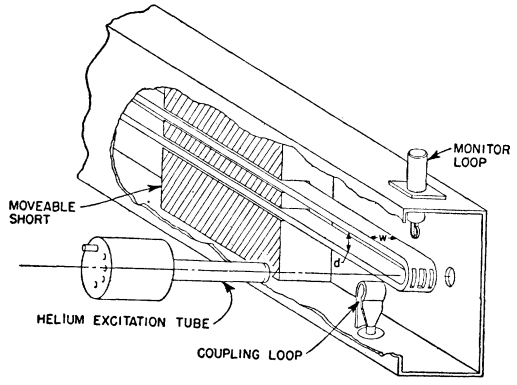

FIG. 10. rf cavity. The dimensions d and w were $\frac{3}{8}$ in. and $\frac{1}{2}$ in. respectively.

[6] J. H. Lees, Proc. Roy. Soc. (London) **137**, 173 (1932).
[7] H. E. Harris, Electronics **24**(1), 130 (1951).

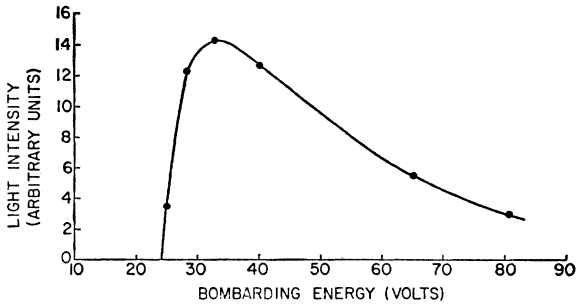

FIG. 11. Typical excitation curve of helium 3889 A collision light as a function of bombarding electron energy.

7. Estimate of rf Magnetic Field Strength

From the geometry of the cavity, which had a measured Q of 750, it was estimated that a power input of 5 w was required to produce an rf magnetic field of 2.8 gauss at the helium tube position.

The rf magnetic field was also monitored indirectly by using a pickup loop (see Fig. 10) located outside the transmission line at a place where the rf magnetic field was about half that present at the end of the line. The induced voltage on the loop could be related by a simple calculation to the rf magnetic field at the helium tube. The fields obtained with this method were in agreement with those obtained by the method involving power input to within a factor two.

IV. OBSERVATIONS AND MEASUREMENTS

1. Excitation Curve and Polarization

The requirements imposed by rf considerations led to the design of a helium tube which was not well suited for determination of good excitation curves and still less for measurement of the polarization of the collision light. Electron dynamics was under little control because of inadequate electron gun design and the possibility of charges on glass walls near the interaction region. Nevertheless, the observed excitation curve of Fig. 11 had very much the expected shape.[6] The polarization measurements may be subject to error because of scattered or reflected light, strains in glass, etc. Although the magnitude of polarization is not of too much significance, the peculiar shape of the observed curve Fig. 12 (contrary to theory as described in reference 1, Sec. IV) is of interest, and will be discussed in a later paper. Observation of helium fine structure resonances was the real goal of the research, and their frequencies may be determined unambiguously even though all characteristics of the polarization are not fully understood.

2. Method of Measurement

The procedure for making a measurement of the resonance field was as follows. The resonance was first located and plotted on the chart recorder by slow change of (modulated) magnetic field, while the rf frequency and amplitude were kept constant. A typical recorder trace is shown in Fig. 13. The center point of the resonance was then found by manually adjusting for a null.

The accuracy of location of a null is limited by noise (assuming a well-defined base line on the chart record) and can be related to the signal-to-noise ratio and resonance width. With the notation of Sec. II2, the signal is

$$\alpha GIS(x,y)/S_{\max}(y),$$

with peak height αGI, and a superimposed noise

$$\alpha GI(S/N)^{-1}.$$

The uncertainty in signal implies an uncertainty in determination of the null by an amount

$$\begin{aligned}\delta x&=(S/N)^{-1}S_{\max}(y)\Big/\left(\frac{\partial S}{\partial x}\right)_{x=0}\\&=[(1+y^2)^2/4y]\cdot(S/N)^{-1}S_{\max}(y).\end{aligned}\tag{10}$$

For $S/N=50$, and optical modulation: $y=y_0=0.577$, $S_{\max}(y_0)=0.65$,

$$\delta x=(4/3)^2\times\tfrac{1}{4}(0.65)/[(0.577)(50)]=0.01,\tag{11}$$

meaning that the null could be located to 1% of ΔH, or to 0.05 gauss if the Lorentzian resonance had a width of 5 gauss.

3. Magnetic Field Measurements

Because of Zeeman splitting of the fine-structure levels, the frequencies of rf transitions depend on magnetic field. According to the discussion in Sec. VI of reference 1, the transitions "5" ($\mathcal{J}=1, m=\pm1\leftrightarrow\mathcal{J}=2, m=\pm1$) have a frequency given by

$$f^2=f_0^2+(g\mu_0H/h)^2.\tag{12}$$

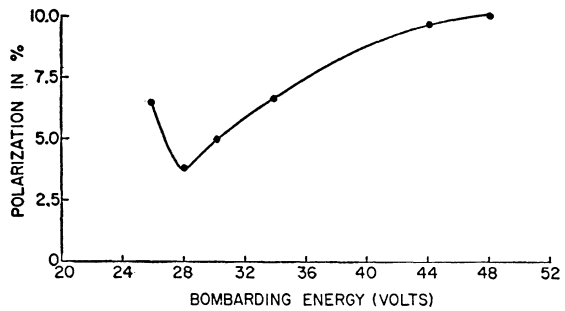

FIG. 12. Typical dependence of the polarization of helium 3889 A collision light as a function of bombarding electron energy.

Here f_0 is the zero-field frequency[8] $J=1\rightarrow J=2$, and $g=g_S-g_L=1.11229$ is the effective Lande g factor.

The electron tubes as constructed did not operate well below 200 gauss, and another feature limited operation between 200 and 350 gauss. By reference to Fig. 2, one sees that in that range of fields the helium resonance is within about 200 Mc/sec of the electron cyclotron resonance frequency. Owing to the presence of a perpendicular component of rf electric field in the interaction space, very broad and intense resonances due to cyclotron action were obtained over this range of magnetic fields instead of the desired helium resonances.

One could hope to utilize these cyclotron resonances for magnetic field measurement, since at very low rf levels they had widths less than one gauss. However, measurable shifts in cyclotron frequency occurred when the beam current or voltage was changed, indicating that dc electric fields existed in the interaction space and disturbed the cyclotron condition so that the method could not be used.

Pending introduction of a nuclear induction method for field measurement, use was made of the known functional form of the helium resonance in order to obtain the magnetic field. Since the magnet was air-cored, a linear relationship between magnet current and magnetic field strength held with high approximation. The magnet current was obtained by measuring the voltage drop across a resistor in series with the magnet, using a type K2 potentiometer. One had then a relation

$$H=a+bP,\tag{13}$$

where a represented any residual field, b is a constant, and P is the potentiometer reading. The value a/b could be found by taking a resonance once in the normal way and again with the magnet current reversed, the difference in potentiometer readings being $2a/b$. A reduced potentiometer reading

$$P_0=P+(a/b)\tag{14}$$

was then calculated in terms of which the frequency of transitions "5" became

$$f^2=f_0^2+(g\mu_0bP_0/h)^2\tag{15}$$

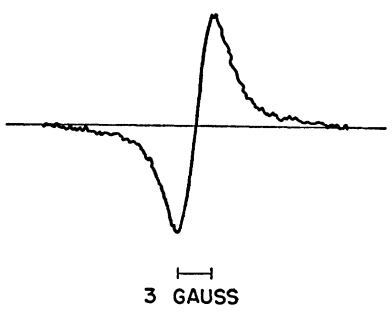

FIG. 13. Typical recording trace of rf resonance curve for transition "5" at a frequency of 900 Mc/sec.

[8] According to the discussion of Sec. XII of reference 1, f_0 includes the shift of $3\,{}^3P_1$ due to singlet-triplet interaction.

so that a plot of f^2 against P_0^2 should yield a straight line with intercept f_0^2.

4. Results

Each set of data led to at least three points to determine the line of Eq. (15). These points were plotted on an extended graph to check for gross deviations, and all of the *a priori* acceptable data showed complete linearity to the accuracy of the graphical plot. The method of least squares was then used to find f_0. Since points could be obtained only between 350 and 600 gauss, considerable extrapolation was required to reach the zero-field intercept. Despite this, however, the results of five sets of data led to f_0 values lying between 657.92 and 658.23 Mc/sec, with an average of 658.0 Mc/sec and an average deviation of 0.09 Mc/sec.

Although the high internal consistency of the data is very encouraging, there were possible uncorrected systematic errors due to (1) inhomogeneity of magnetic field (perhaps 1/300 of the working field) over the effective interaction space, and (2) utilization of small amounts of magnetic materials in construction of the helium tube. These errors will be greatly reduced in future work. The extrapolation method of Sec. IV.3 is less convenient than use of a proton resonance for determination of magnetic field, and will be abandoned. Errors which are well below 0.1 Mc/sec arise from Zeeman curvature, variation of resonance intensity with magnetic field, unsymmetrical square-wave modulation effects, etc.

In view of the above-mentioned possible errors, the separation $3\,^3P_1-3\,^3P_2$ of helium is stated as 658.0 $\pm$1.0 Mc/sec, which is to be compared to the latest optical estimate of 750$\pm$300 Mc/sec. Later papers in this series will deal with the $3\,^3P_0-3\,^3P_1$ separation and the $2\,^3P$ state.

PHYSICAL REVIEW VOLUME 105, NUMBER 2 JANUARY 15, 1957

Thermodynamic Properties of Mixtures on the Statistical Model

J. J. GILVARRY, *The Rand Corporation, Santa Monica, California*

AND

W. G. MCMILLAN, *Department of Chemistry, University of California, Los Angeles, California*

(Received October 8, 1956)

A new method of deriving Brachman's results for the thermodynamic functions of the Thomas-Fermi atom is given in a generalized form applicable to mixtures of electrons and light nuclei in the field of a heavy nucleus.

BRACHMAN[1] has described in outline a method for obtaining the general thermodynamic functions, in particular the Helmholtz free energy F, of the Thomas-Fermi atom at arbitrary temperature based on an integration of the Gibbs-Helmholtz equation. March[2] has pointed out that Brachman's result for the entropy follows directly from the Slater sum, using the distribution function appropriate to a gas of independent electrons at the given local electrostatic potential. In the present discussion we wish to present an alternative derivation of Brachman's results, in which the physical connection between F and the electron chemical potential μ_e occupies a central role, and which applies to somewhat more general systems.

The model to be considered consists of a central heavy nucleus of (large) atomic number Z, surrounded spherically by its complement of Z electrons plus n_s lighter nuclei (e.g., protons) of charge species z_s and their $n_s z_s$ electrons, the whole "molecular" unit being contained in a known spherical volume v at a given temperature T. The coordinate frame will be that of the central nucleus, which otherwise enters only as the source of an external field in which the electrons and the other nuclei move.

For simplicity we shall employ Fermi-Dirac statistics for all particles, writing[3] for the charge density ρ_s due to species s of chemical potential μ_s in a region where the total electrostatic potential is V:

$$\rho_s=(z_s e g_s/h^3)\int_0^\infty \frac{4\pi p^2 dp}{\exp\beta(p^2/2m_s+z_s eV-\mu_s)+1}$$
$$=ez_s\kappa_s I_{\frac{1}{2}}[\beta(\mu_s-z_s eV)], \quad (1)$$

where g_s is the spin degeneracy $2S_s+1$, $\beta=1/kT$, $\kappa_s=2\pi g_s(2m_s/\beta h^2)^{\frac{1}{2}}$, and

$$I_n(\eta)=\int_0^\infty \frac{y^n dy}{\exp(y-\eta)+1}. \quad (2)$$

This is correct in any case for electrons, and makes little error even for boson nuclei as long as the temper-

[1] M. K. Brachman, Phys. Rev. **84**, 1263 (1951).
[2] N. H. March, Phil. Mag. **44**, 346 (1953).
[3] See Feynman, Metropolis, and Teller, Phys. Rev. **75**, 1561 (1949), Sec. V.